Detailed Analytical Modelling of Fractional-Slot Concentrated-Wound Interior Permanent Magnet Machines for Prediction of Torque Ripple

M. Farshadnia, M. A. M. Cheema, R. Dutta, J. E. Fletcher and M. F. Rahman
School of Electrical Engineering and Telecommunications, University of New South Wales, Sydney, Australia
m.farshadnia@unsw.edu.au

***Abstract*—The standard *dq* model of interior permanent magnet machines is based on the assumption of sinusoidal machine parameters. This assumption is flawed especially when a fractional-slot concentrated-wound stator is utilized. In order to address this deficiency, in this paper the non-sinusoidal machine parameters are modelled in the *abc*-system. An extended *dq*-model is then proposed based on the derived non-sinusoidal machine parameters. New parameters are introduced in the proposed model and experimental tests are described for their determination. Based on the proposed extended *dq*-model, detailed equations for the average torque and torque ripple are proposed that specify the parameters involved in the production of different torque components. The proposed extended *dq*-model is used to predict the performance of a prototype fractional-slot concentrated-wound interior permanent magnet machine.**

***Keywords*—Torque ripple; inductance harmonics; dq model; Permanent magnet machine; fractional-slot concentrated-wound stator.**

I. Introduction

Compared with distributed-wound (DW) interior permanent magnet (IPM) machines, fractional-slot concentrated-wound (FSCW) IPM machines are more apt for compact and high power density drive systems. In such drive systems, an exact electrical model of the machine can facilitate in obtaining a smooth output torque under different operating conditions.

The key elements in the electric model of a permanent magnet (PM) synchronous machine (PMSM) are the PM flux linkages and the self- and mutual inductances. These parameters result from the interaction of the rotor PM flux density and the rotor airgap function with the stator magneto-motive force (MMF), respectively. In the standard *dq* model of PMSMs, the machine parameters are assumed sinusoidal, leading to constant PM flux linkages and inductances in the *d*- and *q*-axes and a smooth electromagnetic torque [1, 2]. This assumption is only valid in a perfect DW stator where the spatial distribution of each phase winding in the stator is sinusoidal, leading to a sinusoidal MMF. In the case of a FSCW stator, the generated MMF is non-sinusoidal and contains a wide range of spatial harmonics as shown in Fig. 1 for an example FSCW PMSM. This causes the machine parameters to become non-sinusoidal, which in turn yield to ripples in the electromagnetic torque [3-6]. In such a case, evaluation of the machine performance based on the standard *dq* model yields false results [7]. This necessitates a *dq* model for FSCW PMSMs that takes into account the non-sinusoidal machine parameters.

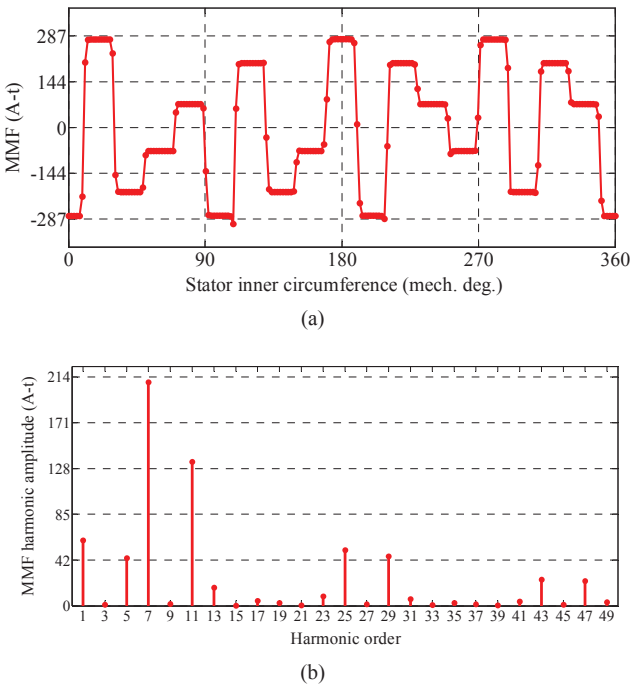

Fig. 1. Field characteristics of a 14-pole 18-slot FSCW PMSM obtained using finite-element analysis. (a) MMF spatial waveform at an arbitrary moment. (b) Harmonic spectrum of the MMF showing the dominant 7th harmonic.

Methods for analytical modeling PMSMs in the literature lack a mathematical interpretation for the effect of the non-sinusoidal machine parameters on its performance [8-11]. In particular, a comprehensive mathematical model for the electromagnetic torque and its ripple as a function of the machine non-sinusoidal parameters is yet to be proposed.

In order to fill the aforementioned gap in the literature, an extended *dq* model for FSCW PMSMs is proposed in this paper which accounts for the non-sinusoidal machine parameters. To this aim, the PM flux linkages and self- and mutual inductances of the machine are formulated in the *abc*-system to form the machine dynamic voltage equations which are then transformed to the *qd0*-reference frame. New parameters are introduced in the proposed extended *dq* model and methods for their experimental measurement are presented. The proposed extended *dq* model is used to derive detailed expressions for the average torque and the torque ripple. The generated electromagnetic torque is classified into subcomponents, each of them a function of the newly introduced parameters in the extended *dq* model. The proposed extended *dq* model is applied to a prototype FSCW

978-1-5090-07370/16/$31.00 ©2016 Crown

PMSM in the laboratory; its parameters are experimentally measured and used to predict the machine's electromagnetic torque.

II. Standard *dq* Model of PMSMs

The voltage equations of a PMSM in the *abc*-system are given as [1]:

$$\mathbf{v}_{abc} = \mathbf{r}_s \mathbf{i}_{abc} + \frac{d\,\boldsymbol{\lambda}_{abc}}{dt} \tag{1}$$

$$\boldsymbol{\lambda}_{abc} = \mathbf{L}_s \mathbf{i}_{abc} + \boldsymbol{\lambda}_{pm,abc} \tag{2}$$

where $\mathbf{v}_{abc}$, $\mathbf{i}_{abc}$, and $\boldsymbol{\lambda}_{abc}$ represent the column vectors of the stator voltages, currents, and flux linkages, respectively, $\mathbf{r}_s$ is a diagonal matrix comprised of the stator resistance, $\boldsymbol{\lambda}_{pm,abc}$ is a column vector comprised of the PM flux linkages, and $\mathbf{L}_s$ is the three-phase inductance matrix. In a perfect DW machine, the PM flux linkages and the inductances are sinusoidal

The PM flux linkages in a PMSM with a perfect DW stator are sinusoidal and given by:

$$\boldsymbol{\lambda}_{pm,abc} = \begin{bmatrix} \lambda_{pm,a}(\theta_m) & \lambda_{pm,b}(\theta_m) & \lambda_{pm,c}(\theta_m) \end{bmatrix}^{\mathrm{T}} \tag{3}$$

where the superscript "T" indicates the transpose operator, and $\lambda_{pm,x}$ represents the PM flux linkage of phase x and is a function of the rotor angular position in electrical radians, θ_m, given by:

$$\lambda_{pm,x}(\theta_m) = \lambda_{pm} \sin\left(\theta_m + \theta_x\right) \tag{4}$$

and

$$\theta_m = \omega_m\, t \tag{5}$$

where ω_m is the rotational speed of the rotor in electrical rad/s, λ_{pm} is the PM flux linkage amplitude, and θ_x is spatial phase displacement of the machine phase windings and is equal to 0, $-2\pi/3$ and $+2\pi/3$, for phase a, b, and c, respectively.

The three-phase inductance matrix in (2) is given by [1]:

$$\mathbf{L}_s = \begin{bmatrix} L_a(\theta_m) & M_{ab}(\theta_m) & M_{ac}(\theta_m) \\ M_{ab}(\theta_m) & L_b(\theta_m) & M_{bc}(\theta_m) \\ M_{ac}(\theta_m) & M_{bc}(\theta_m) & L_c(\theta_m) \end{bmatrix} \tag{6}$$

In (6), L_x is the self-inductance of phase x, and M_{xy} is the mutual inductance between phase x and y. In a perfect DW machine, the self- and mutual inductances are sinusoidal, and a function of the rotor angular position in electrical radians, θ_m, expressed by:

$$L_x(\theta_m) = L_{ls} + L_0 + L_2 \cos 2(\theta_m - \theta_x) \tag{7}$$

$$M_{xy}(\theta_m) = -\frac{1}{2} L_0 + L_2 \cos 2(\theta_m - \theta_{xy}) \tag{8}$$

where L_{ls} is the leakage inductance, L_0 and L_2 are the average value and the second spatial harmonic amplitude of the self-inductance, and θ_{xy} is a spatial phase displacement and for phases ab, ac, and bc equals to to $-\pi/3$, $+\pi/3$, and π, respectively. Equations (1)-(8) comprise the dynamic model of a PMSM with a perfect DW stator in the *abc*-system.

The machine model in the *abc*-system can be transformed to the *qd0*-reference frame using the Park transformation matrix, expressed by [12]:

$$\mathbf{K}_s = \frac{2}{3} \begin{bmatrix} \cos\theta_m & \cos(\theta_m - \frac{2\pi}{3}) & \cos(\theta_m + \frac{2\pi}{3}) \\ \sin\theta_m & \sin(\theta_m - \frac{2\pi}{3}) & \sin(\theta_m + \frac{2\pi}{3}) \\ 1/2 & 1/2 & 1/2 \end{bmatrix} \tag{9}$$

Multiplying both sides of (1) and (2) by (9) yields:

$$\mathbf{v}_{qd0} = \mathbf{r}_s \mathbf{i}_{qd0} + \omega_m\, \boldsymbol{\lambda}_{dq} + \frac{d\,\boldsymbol{\lambda}_{qd0}}{dt} \tag{10}$$

$$\boldsymbol{\lambda}_{qd0} = \mathbf{L}_{qd0} \mathbf{i}_{qd0} + \boldsymbol{\lambda}_{pm,qd0} \tag{11}$$

where

$$\boldsymbol{\lambda}_{dq} = \begin{bmatrix} \lambda_d & -\lambda_q & 0 \end{bmatrix}^{\mathrm{T}}. \tag{12}$$

The PM flux linkage column vector, $\boldsymbol{\lambda}_{pm,qd0}$, and the inductance matrix, $\mathbf{L}_{qd0}$, in the *qd0*-reference frame are given by:

$$\mathbf{L}_{qd0} = diag\begin{bmatrix} L_q & L_d & L_0 \end{bmatrix} \tag{13}$$

$$\boldsymbol{\lambda}_{pm,qd0} = \begin{bmatrix} 0 & 1 & 0 \end{bmatrix}^{\mathrm{T}} \tag{14}$$

where *diag* stands for a diagonal matrix and

$$L_q = L_{ls} + \frac{3}{2}(L_0 + L_2) \tag{15}$$

$$L_d = L_{ls} + \frac{3}{2}(L_0 - L_2) \tag{16}$$

$$L_0 = L_{ls} \tag{17}$$

From the standard *dq* model, and by neglecting the resistive losses, electromagnetic torque for a P pole PMSM, as a function of the *qd0* currents is given by [12]:

$$T_e = \frac{3}{2}\frac{P}{2}\left(\lambda_d i_q - \lambda_q i_d\right) \tag{18}$$

Substituting λ_d and λ_q from (11) in (18) yields:

$$T_e = \frac{3}{2}\frac{P}{2}\left(\lambda_{pm}\, i_q + (L_d - L_q) i_q\, i_d\right) \tag{19}$$

The first term in (19) represents the field-alignment torque and originates from the interaction between the PM flux density and stator MMF. The second term in the above equation is the reluctance torque and is generated due to the machine saliency.

III. Proposed Extended *dq* Model for FSCW PMSMs

FSCW PMSMs have a non-sinusoidal spatial MMF distribution in the airgap which is determined based on the simplest fraction describing the machine's slots-per-pole-per-phase value, S_{pp}. An IPM rotor which is characterized by a variable permeance function and a non-sinusoidal PM flux density is considered in this section as a general case. The PM flux linkages and inductances in such a machine are non-sinusoidal and should be carefully modelled in the *abc*-system for use in (1) and (2).

A. Detailed Expressions for the PM Flux Linkage and Self- and Mutual Inductances in the abc-System

The PM flux linkage of phase x is the result of the interaction between the winding function, w_x, and the PM

flux density, B_{pm}, given by [1]:

$$\lambda_{pm,x}(\theta_m) = r_g\, l_{eff} \int_0^{2\pi} w_x(\theta_s)\; B_{pm}(\theta_m, \theta_s)\; d\theta_s \quad (20)$$

where r_g is the mean airgap radius, l_{eff} is the effective length of the machine, and θ_s is the angle subtended along the stator circumference.

Winding function of phase x is described as the MMF produced by that phase when carrying unity current, described using Fourier series as [4]:

$$w_x(\theta_s) = \sum_n^{\infty} W_n \cos(n\theta_s + n\theta_x)\,, \quad n = \frac{P}{2c}, \frac{3P}{2c}, \frac{5P}{2c}, \ldots \quad (21)$$

where W_n is the amplitude of the n^{th} spatial harmonic of the winding function, and c is the denominator in S_{pp}. General equations for calculation the winding function harmonic amplitudes for FSCW stator topologies are given in [4].

PM flux density of an IPM rotor is in the form of a trapezoid and for a rotary rotor can be described using Fourier series as [4]:

$$B_{pm}(\theta_m, \theta_s) = \sum_n^{\infty} B_n \sin(n\theta_m / (P/2) - n\theta_s)\,, \quad n = \frac{P}{2}, \frac{3P}{2}, \frac{5P}{2}, \ldots \quad (22)$$

where B_n is the amplitude of the n^{th} spatial harmonic of the PM flux density. Substitution of (21) and (22) in (20) and solving the integral yields the PM flux linkage of phase x in the following general form:

$$\lambda_{pm,x}(\theta_m) = \sum_{n=1,\,3,\,5,\,\ldots}^{\infty} \lambda_{pm,n} \sin\left(n\theta_m - n\theta_x\right) \quad (23)$$

From (23) it is concluded that the PM flux linkage in an FSCW PMSM comprises odd spatial harmonics.

The self- and mutual inductances of a synchronous machine are given by [1]:

$$L_x(\theta_m) = \int_0^{2\pi} w_x^2(\theta_s) C(\theta_m, \theta_s) d\theta_s \quad (24)$$

$$M_{xy}(\theta_m) = \int_0^{2\pi} w_x(\theta_s) w_y(\theta_s) C(\theta_m, \theta_s) d\theta_s \quad (25)$$

In (24) and (25), C is the permeance function and is used to describe the permeance of the stator flux path with respect to the rotor position. This function can be formulated using Fourier series as the following general form [13]:

$$C(\theta_m, \theta_s) = C_0 + \sum_n^{\infty} C_n \cos(n\theta_m / (P/2) - n\theta_s)\,, \quad n = P,\, 2P,\, 3P,\, \ldots \quad (26)$$

where C_0 is the average value, and C_n is the amplitude of the n^{th} spatial harmonic of the permeance function.

Substitution of (21) and (26) in (24) and (25), and solving the integrals yields detailed expressions for the self- and mutual inductances which can be cumulated in the following general forms:

$$L_x(\theta_m) = L_0 + \sum_{n=2,4,6,\ldots}^{\infty} L_n \cos(n\theta_m - n\theta_x) \quad (27)$$

$$M_{xy}(\theta_m) = M_0 + \sum_{n=2,4,6,\ldots}^{\infty} M_n \cos(n\theta_m - n\theta_{xy}) \quad (28)$$

where, L_n is the n^{th} harmonic of the self-inductance, M_0 is the average value of the mutual inductance, and M_n is the n^{th} harmonic of the mutual inductance. Most electric machines are designed to operate close to the magnetic saturation knee of the magnetic material used in their construction to have the maximum power density. Consequently, the saturation level of the iron core varies with the current level, leading to a change in the permeance function of the flux path, (26). Subsequently, based on (24)-(25), L_0 , M_0 , L_n, and M_n in the self- and mutual inductances become functions of the current amplitude. From (27) and (28) it is observed that only even harmonics exist in the inductance matrix of an FSCW PMSM.

The detailed model for an FSCW PMSM with a non-salient rotor in the *abc*-system is described by (1)-(3), (6), (23), (27) and (28).

B. Transformation of the Detailed Machine Model from the abc-system to the qd0-reference frame

Park transformation matrix, (9), is used to transform the detailed machine model from the *abc*-system to the *qd0*-reference frame. This yields voltage and flux linkage equations similar to (10)-(12), however, the PM flux linkage column vector and the inductance matrix should be modified according to their detailed expressions as derived in the following.

Transformation of the detailed PM flux linkage column vector described by (3) and (23) from the *abc*-system to the *qd0*-reference frame yields:

$$\boldsymbol{\lambda}_{pm,qd0} = \left[\lambda_{pm,q}(\theta_m) \quad \lambda_{pm,d}(\theta_m) \quad \lambda_{pm,0}(\theta_m)\right]^{\mathrm{T}} \quad (29)$$

where

$$\lambda_{pm,q}(\theta_m) = \sum_{n=6k} \lambda_{pm,q,n} \sin(n\theta_m)\,, \quad k = 1,2,3,\ldots \quad (30)$$

$$\lambda_{pm,d}(\theta_m) = \lambda_{pm,d,0}\,, \quad k = 1,2,3,\ldots \quad -\sum_{n=6k} \lambda_{pm,d,n} \cos(n\theta_m) \quad (31)$$

$$\lambda_{pm,0}(\theta_m) = \sum_{n=3k} \lambda_{pm,0,n} \sin(n\theta_m)\,, \quad k = 1,3,5,\ldots \quad (32)$$

and

$$\lambda_{pm,q,n} = \lambda_{pm,n-1} + \lambda_{pm,n+1} \quad (33)$$

$$\lambda_{pm,d,0} = \lambda_{pm,1} \quad (34)$$

$$\lambda_{pm,d,n} = \lambda_{pm,n-1} - \lambda_{pm,n+1} \quad (35)$$

$$\lambda_{pm,0,n} = \lambda_{pm,n}\,. \quad (36)$$

Evidently the *d*-axis PM flux linkage comprises an average value superimposed by spatial harmonics of order $6k$, $k = 1, 2, 3, \ldots$. The *q*- and 0-axis PM flux linkages have a zero average value with spatial harmonics of order $6k$, $k = 1, 2, 3, \ldots$, and $3k$, $k = 1, 3, 5, \ldots$, respectively.

Transformation of the detailed inductance matrix

described by (6), (27), and (28) from the *abc*-system to the *qd0*-reference frame yields:

$$\mathbf{L}_{qd0} = \begin{bmatrix} L_q(\theta_m) & M_{qd}(\theta_m) & M_{q0}(\theta_m) \\ M_{qd}(\theta_m) & L_d(\theta_m) & M_{d0}(\theta_m) \\ M_{0q}(\theta_m) & M_{0d}(\theta_m) & L_0(\theta_m) \end{bmatrix}. \quad (37)$$

where the diagonal elements are the self-inductances of the *q*-, *d*-, and 0-axes, and the non-diagonal elements are the mutual inductances between the *q*-, *d*-, and 0-axes.

The self-inductances in (37) are derived as follows:

$$L_q(\theta_m) = L_{q,0} + \sum_{n=6k} L_{q,n}\cos(n\theta_m) \quad , \quad k = 1,2,3,... \quad (38)$$

$$L_d(\theta_m) = L_{d,0} + \sum_{n=6k} L_{d,n}\cos(n\theta_m) \quad , \quad k = 1,2,3,... \quad (39)$$

$$L_0(\theta_m) = L_{0,0} + \sum_{n=6k} L_{0,n}\cos(n\theta_m) \quad , \quad k = 1,2,3,... \quad (40)$$

where

$$L_{q,0} = (L_0 - M_0) + \frac{1}{2}(L_2 + 2M_2) \quad (41)$$

$$L_{q,n} = \frac{1}{2}\{(L_{n-2} + 2M_{n-2}) + 2(L_n - M_n) + (L_{n+2} + 2M_{n+2})\} \quad (42)$$

$$L_{d,0} = (L_0 - M_0) - \frac{1}{2}(L_2 + 2M_2) \quad (43)$$

$$L_{d,n} = -\frac{1}{2}\{(L_{n-2} + 2M_{n-2}) - 2(L_n - M_n) + (L_{n+2} + 2M_{n+2})\} \quad (44)$$

$$L_{0,0} = L_0 + 2M_0 \quad (45)$$

$$L_{0,n} = L_n + 2M_n \, . \quad (46)$$

The mutual inductances in (37) are found to be:

$$M_{qd}(\theta_m) = \sum_{n=6k} M_{qd,n}\sin(n\theta_m) \quad , \quad k = 1,2,3,... \quad (47)$$

$$M_{q0}(\theta_m) = \sum_{n=3k} M_{q0,n}\sin(n\theta_m) \quad , \quad k = 1,3,5,... \quad (48)$$

$$M_{d0}(\theta_m) = \sum_{n=3k} M_{d0,n}\sin(n\theta_m) \quad , \quad k = 1,3,5,... \quad (49)$$

$$M_{0q}(\theta_m) = \frac{1}{2}M_{q0}(\theta_m) \quad (50)$$

$$M_{0d}(\theta_m) = \frac{1}{2}M_{d0}(\theta_m) \quad (51)$$

where

$$M_{qd,n} = \frac{1}{2}\{(L_{n-2} + 2M_{n-2}) - (L_{n+2} + 2M_{n+2})\} \quad (52)$$

$$M_{q0,n} = (L_{n-1} - M_{n-1}) + (L_{n+1} - M_{n+1}) \quad (53)$$

$$M_{d0,n} = (L_{n-1} - M_{n-1}) - (L_{n+1} - M_{n+1}) \, . \quad (54)$$

From (38)-(40), the *qd0* self-inductances comprise an average value superimposed by spatial harmonics of order 6*k*, $k = 1, 2, 3, \ldots$. The *qd0* mutual inductances described by (47)-(49) have a zero average value and comprise spatial harmonics of order 6*k*, $k = 1, 2, 3, \ldots$ for M_{qd} and 3*k*, $k = 1, 3, 5, \ldots$ for M_{0q} and M_{0d}.

Evidently, in contrast with the standard *dq* model, in the detailed *dq* model, the PM flux linkages and the inductances in the *qd*0-reference frame are a function of the rotor angular position. Moreover, the non-diagonal elements in the *qd0* inductance matrix are non-zero.

C. Formulation of the Proposed Extended dq Model

The extended *dq* model of the FSCW PMSM is found by substituting the detailed PM flux linkage column vector and detailed inductance matrix in (10) and (11):

$$\mathbf{v}_{qd0} = \mathbf{r}_s\,\mathbf{i}_{qd0} + \omega_m \boldsymbol{\lambda}_{dq} + \frac{d\,\mathbf{L}_{qd0}}{dt}\mathbf{i}_{qd0} + \mathbf{L}_{qd0}\frac{d\,\mathbf{i}_{qd0}}{dt} + \frac{d\,\boldsymbol{\lambda}_{pm,qd0}}{dt} \quad (55)$$

and

$$\boldsymbol{\lambda}_{dq} = \begin{bmatrix} \lambda_d(\theta_m) & -\lambda_q(\theta_m) & 0 \end{bmatrix}^{\mathrm{T}} \quad (56)$$

Manipulating (55) yields the extended *dq* model of the FSCW PMSM:

$$v_q = r_s\,i_q + \omega_m \lambda_d(\theta_m) + L_q(\theta_m)\frac{di_q}{dt} + v_{\Delta L,q} + v_{\Delta\lambda,q} + v_{\Delta i,q} \quad (57)$$

$$v_d = r_s\,i_d - \omega_m \lambda_q(\theta_m) + L_d(\theta_m)\frac{di_d}{dt} + v_{\Delta L,d} + v_{\Delta\lambda,d} + v_{\Delta i,d} \quad (58)$$

$$v_0 = r_s\,i_0 + L_0(\theta_m)\frac{di_0}{dt} + v_{\Delta L,0} + v_{\Delta\lambda,0} + v_{\Delta i,0} \quad (59)$$

In (57), $v_{\Delta L,q}$ is the induced voltage in the *q*-axis due to the rotor position dependency of L_q, M_{qd} and M_{q0},

$$v_{\Delta L,q} = \frac{dL_q(\theta_r)}{dt}i_q + \frac{dM_{qd}(\theta_r)}{dt}i_d + \frac{dM_{q0}(\theta_r)}{dt}i_0 \quad (60)$$

$v_{\Delta\lambda,q}$ is the is the induced voltage in the *q*-axis due to the rotor position dependency of the *q*-axis PM flux density:

$$v_{\Delta\lambda,q} = \frac{d\,\lambda_{pm,q}}{dt} \quad (61)$$

and $v_{\Delta i,q}$ is the induced voltage in the *q*-axis due to the time dependency of the d- and 0-axes currents:

$$v_{\Delta i,q} = M_{qd}(\theta_r)\frac{di_d}{dt} + M_{q0}(\theta_r)\frac{di_0}{dt} \, . \quad (62)$$

Similarly, $v_{\Delta L,d}$, $v_{\Delta\lambda,d}$ and $v_{\Delta i,d}$ for the d-axis and $v_{\Delta L,0}$, $v_{\Delta\lambda,0}$ and $v_{\Delta i,0}$ for the 0-axis are given by:

$$v_{\Delta L,d} = \frac{dM_{qd}(\theta_r)}{dt}i_q + \frac{dL_d(\theta_r)}{dt}i_d + \frac{dM_{d0}(\theta_r)}{dt}i_0 \quad (63)$$

$$v_{\Delta\lambda,d} = \frac{d\,\lambda_{pm,\mathrm{d}}}{dt} \quad (64)$$

$$v_{\Delta i,d} = M_{qd}(\theta_r)\frac{di_q}{dt} + M_{d0}(\theta_r)\frac{di_0}{dt} \quad (65)$$

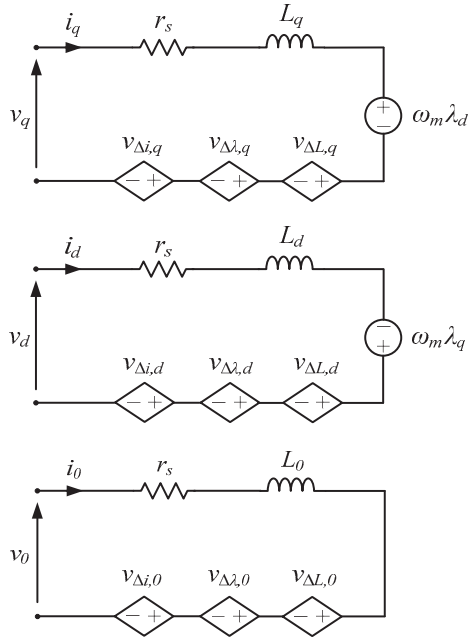

Fig. 2. FSCW PMSM equivalent circuit based on the extended *dq* model.

$$v_{\Delta L,0} = \frac{dM_{0q}(\theta_r)}{dt} i_q + \frac{dM_{0d}(\theta_r)}{dt} i_d + \frac{dL_0(\theta_r)}{dt} i_0 \tag{66}$$

$$v_{\Delta\lambda,0} = \frac{d\lambda_{pm,0}}{dt} \tag{67}$$

$$v_{\Delta i,0} = M_{0q}(\theta_r)\frac{di_q}{dt} + M_{0d}(\theta_r)\frac{di_d}{dt}. \tag{68}$$

Equivalent circuit of the FSCW PMSM based on the proposed extended *dq* model is shown in Fig. 2.

D. Detailed Formulation of Electromagnetic Torque using the Proposed Extended dq Model

The instantaneous active power in the *qd0*-reference frame is expressed by [1]:

$$p = \frac{3}{2}\left(v_q i_q + v_d i_d + 2v_0 i_0\right). \tag{69}$$

Substitution of v_q, v_d and v_0 from the proposed extended *dq* model in (69) with a few steps of mathematical manipulations yields:

$$\begin{aligned} p = \frac{3}{2}\Bigg[& \left(r_s i_q^2 + r_s i_d^2 + 2r_s i_0^2\right) + \omega_m\left(\lambda_d i_q - \lambda_q i_d\right) \\ & + \omega_m\begin{bmatrix} i_q & i_d & 2i_0 \end{bmatrix}\left(\frac{d\,\mathbf{L}_{qd0}}{d\theta_m}\mathbf{i}_{qd0} + \frac{d\boldsymbol{\lambda}_{pm,qd0}}{d\theta_m}\right) \\ & + \begin{bmatrix} i_q & i_d & 2i_0 \end{bmatrix}\mathbf{L}_{qd0}\frac{d\,\mathbf{i}_{qd0}}{dt}\Bigg] \end{aligned} \tag{70}$$

The first term in (70) indicates the resistive losses, the second and third terms in (70) are the powers that participates in the energy conversion process, and the last term is the rate of change of the stored energy in the magnetic field due to variations in the current amplitude.

In steady-state condition, the electromagnetic torque in a FSCW PMSM can be obtained by dividing the second and third terms in (70) by the rotational speed [14, 15]:

$$\begin{aligned} T_e = \frac{3}{2}\frac{P}{2}\Bigg[& \left(\lambda_d i_q - \lambda_q i_d\right) \\ & + \begin{bmatrix} i_q & i_d & 2i_0 \end{bmatrix}\left(\frac{d\,\mathbf{L}_{qd0}}{d\theta_r}\mathbf{i}_{qd0} + \frac{d\boldsymbol{\lambda}_{pm,qd0}}{d\theta_r}\right)\Bigg] \end{aligned} \tag{71}$$

Substitution of the detailed equations of the flux linkages and inductances into the above equation gives:

$$T_e = T_{ave} + T_{r,\lambda} + T_{r,rel} \tag{72}$$

where T_{ave} is the average electromagnetic torque, $T_{r,\lambda}$ is the field-alignment torque ripple due to the PM flux linkages, and $T_{r,rel}$ is the reluctance torque ripple due to the machine saliency, and can be expressed in detailed form as follows:

$$T_{ave} = \frac{3}{2}\frac{P}{2}\left(\lambda_{pm,d,0} i_q + (L_{d,0} - L_{q,0}) i_q i_d\right) \tag{73}$$

$$\begin{aligned} T_{r,\lambda} = -\frac{3}{2}\frac{P}{2}\Bigg\{ & i_q \sum_{n=6,12,18,\ldots}\left(\lambda_{pm,d,n} - n\lambda_{pm,q,n}\right)\cos(n\theta_m) \\ & + i_d \sum_{n=6,12,18,\ldots}\left(\lambda_{pm,q,n} - n\lambda_{pm,d,n}\right)\sin(n\theta_m) \\ & - 2i_0 \sum_{n=3,9,15,\ldots} n\lambda_{pm,0,n}\cos(n\theta_m)\Bigg\} \end{aligned} \tag{74}$$

$$\begin{aligned} T_{r,rel} = \frac{3}{2}\frac{P}{2}\Bigg\{ & (i_q^2 - i_d^2)\sum_{n=6,12,18,\ldots} M_{qd,n}\sin(n\theta_m) \\ & - \sum_{n=6,12,18,\ldots} n(L_{q,n} i_q^2 + L_{d,n} i_d^2 + 2L_{0,n} i_0^2)\sin(n\theta_m) \\ & + i_0 \sum_{n=1,9,15,\ldots}(M_{d0,n} i_q - M_{q0,n} i_d)\sin(n\theta_m) \\ & + i_q i_d \sum_{n=6,12,18,\ldots}(L_{d,n} - L_{q,n} + 2nM_{qd,n})\cos(n\theta_m) \\ & + 2i_0 \sum_{n=3,9,15,\ldots} n(M_{q0,n} i_q + M_{d0,n} i_d)\cos(n\theta_m)\Bigg\} \end{aligned} \tag{75}$$

The first term in the average torque (73) is the field-alignment torque while the second term is the reluctance torque. It is observed that the average field-alignment torque originates from the average value of the *d*-axis PM flux linkage, while the average reluctance torque is produced by the average values of the *d*- and *q*-axis inductances.

Equations (74) and (75) imply that torque ripple in a FSCW PMSM is due to the spatial harmonics of the *qd0* PM flux linkages and inductances. The torque ripple is composed of two groups of harmonics with their order being n = 6, 12, 18, … and n = 3, 9, 15, …. The latter group only exists if the zero sequence currents are circulating in the system.

IV. Tests for Determination of the Parameters in the Proposed Extended *dq* Model

The parameters of the proposed extended *dq* model comprise the *qd0* PM flux linkages and inductances. From (30)-(36) and (38)-(54), these parameters are calculated using the harmonics of the detailed PM flux linkages and detailed self- and mutual inductances in the *abc*-system. Experimental tests are introduced in this section for measuring these parameters.

A. Measurement of the PM Flux Linkage Harmonics

According to Faraday's law, back-EMF of phase x is obtained from the derivative of the associated PM flux linkage. Thereby, PM flux linkage harmonics can be found by measuring the phase-to-neutral back-EMF harmonics. From (23), for a machine that rotates at the speed ω_m in electrical rad/s, phase-to-neutral back-EMF is expressed by:

$$e_x(t) = -\frac{d}{dt}\left(\sum_{n}^{\infty} \lambda_{pm,n} \sin(n\omega_m t - n\theta_x)\right) = -\sum_{n=1,3,5,\ldots}^{\infty} \underbrace{n\omega_m \lambda_{pm,n}}_{E_n} \cos(n\omega_m t - n\theta_x) \tag{76}$$

where E_n is the peak of the n^{th} harmonic of the back-EMF. Thus the PM flux linkage harmonic of order n can be obtained by:

$$\lambda_{pm,n} = \frac{E_n}{n\omega_m} \quad , \qquad n = 1,\ 3,\ 5,\ \ldots \tag{77}$$

By measuring the back-EMF harmonics at rotational speed ω_m, PM flux linkage harmonics for use in the extended dq model can be found from (77).

B. Measurement of the Self- and Mutual Inductances

The spatial waveforms of the self- and mutual inductances as a function of the rotor position can be measured using the AC standstill test [16]. In this method, an arbitrary phase winding of the machine is supplied with a constant AC current, while the two other phases remain open circuit. The rotor is locked at different angular positions in one electrical cycle and the three-phase voltages are measured. In each rotor position, the value of the self- and mutual inductances can be found from:

$$L_x = \frac{\sqrt{(V_x/I_x)^2 - r_s^2}}{2\pi f} \tag{78}$$

$$M_{xy} = \frac{V_y}{2\pi f I_x} \tag{79}$$

where V_x and V_y are the line-to-neutral rms voltages of phase x and y, respectively, I_x is the rms current in phase x, and f is the supply frequency.

Once the AC standstill test is performed for one electric cycle, the average value and the harmonics of the inductances can be found by performing an FFT analysis on the obtained spatial inductance waveforms.

V. Experimental Results and Discussion

In this section, the parameters of the proposed extended dq model are measured for a 1kW, 2.55Arms 14-pole 18-slot prototype FSCW IPM machine with its design parameters as described in [17]. These parameters are then used to estimate the average torque and torque ripple for the prototype machine.

A. Measurement of the Extended dq-model Parameters

The PM flux linkage harmonics of the test machine in the abc-system are obtained using the approach detailed in Section IV.A. To this aim, the back-EMF is first measured at the synchronous speed as shown in Fig. 3. The measured harmonic content of the back-EMF for phase a and the associated PM flux linkages calculated using (77) are listed in Table I. The data of this table is used in (30)-(36) to obtain the detailed PM flux linkages in the $qd0$-reference frame as shown in Fig. 4. Evidently, harmonics are present in the $qd0$ PM flux linkage spatial waveforms resulting in variations of the PM flux linkages with the rotor position. Among the $qd0$ PM flux linkages of Fig. 4, only the d-axis PM flux linkage has a non-zero mean value.

The self- and mutual inductances of the test machine are measured using the AC standstill test as explained in Section IV.B for five current levels: 1Arms, 1.4Arms, 1.8Arms, 2.2Arms, 2.5Arms. The spatial waveform of the inductances as a function of the rotor position are shown in Fig. 5.

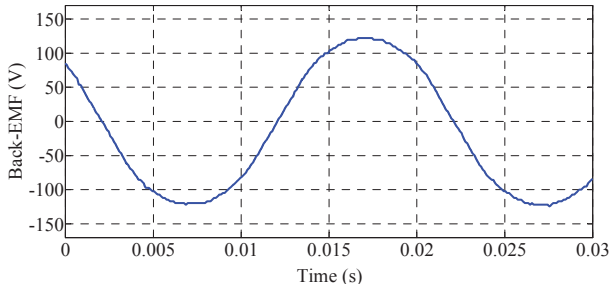

Fig. 3. Measured back-EMF of the prototype FSCW PMSM.

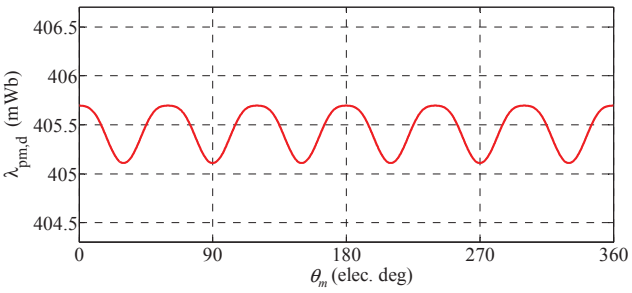

(a)

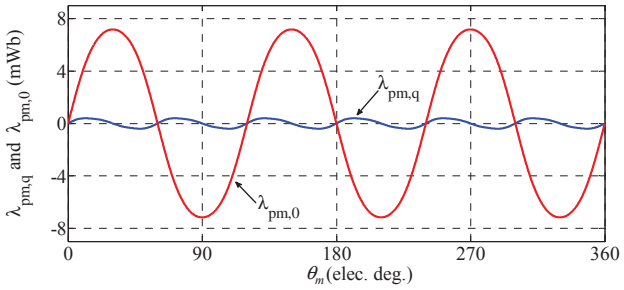

(b)

Fig. 4. PM flux linkages of the extended dq model for the prototype FSCW PMSM. (a) d-axis PM flux linkage. (b) q-axis and 0 -axis PM flux linkages.

TABLE I
Harmonic Content of the Measured PM Flux Linkage

	Harmonic Order					
	0	1	3	5	7	9
E_a (V)	0	127.38	7.06	0.08	0.07	
$\lambda_{pm,a}$ (mWb)	0	405.48	7.49	0.05	0.35	0.32

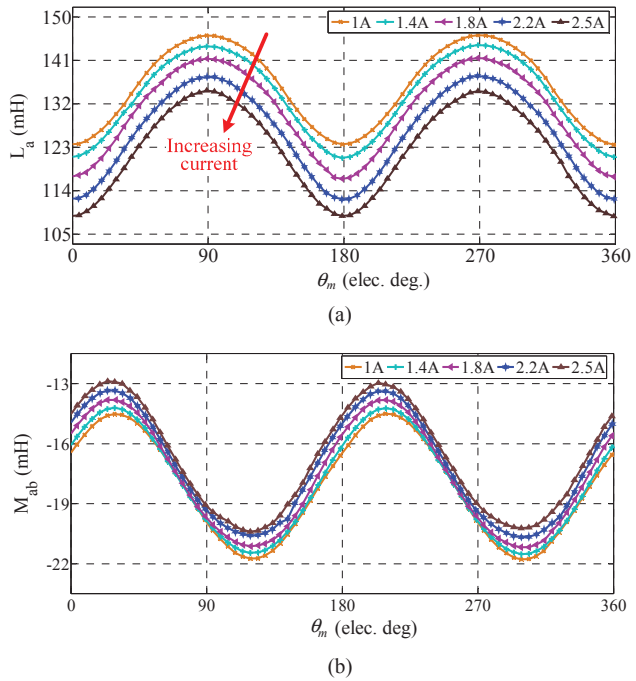

Fig. 5. Measured inductances of the prototype FSCW PMSM at different current excitation conditions. (a) Self-inductance. (b) Mutual inductance.

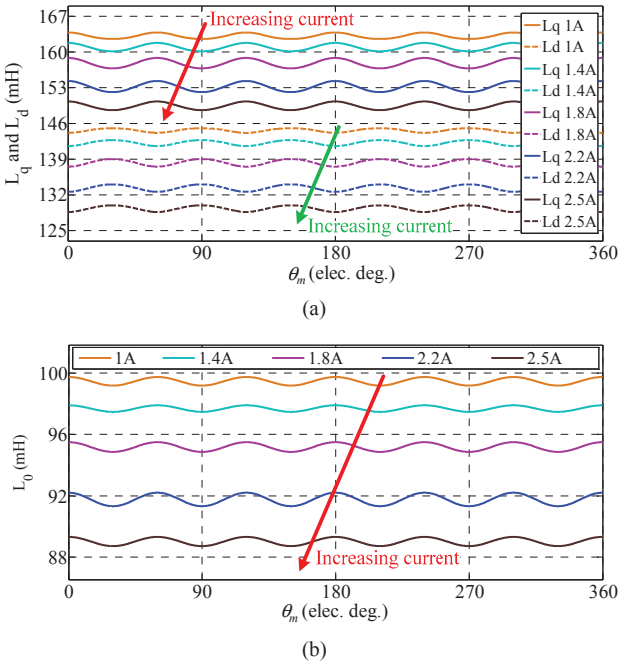

Fig. 6. Diagonal elements in the inductance matrix in the proposed extended *dq* model. (a) *d*-axis and *q*-axis self-inductances. (b) 0-axis self-inductance.

TABLE I
HARMONIC CONTENT OF THE MEASURED SELF- AND MUTUAL INDUCTANCES

Inductance (mH)	HARMONIC ORDER				
	dc	2	4	6	8
L_a 1A	135.742	11.322	0.902	0.161	0.068
L_a 1.4A	133.594	11.489	1.141	0.153	0.014
L_a 1.8A	130.421	12.068	1.371	0.213	0.057
L_a 2.2A	126.112	12.446	1.240	0.261	0.106
L_a 2.5A	122.614	12.676	0.987	0.160	0.117
M_{ab} 1A	-18.15	3.568	0.022	0.006	0.003
M_{ab} 1.4A	-17.955	3.609	0.107	0.003	0.014
M_{ab} 1.8A	-17.622	3.685	0.165	0.059	0.002
M_{ab} 2.2A	-17.175	3.674	0.203	0.089	0.003
M_{ab} 2.5A	-16.789	3.685	0.184	0.071	0.002

Evidently, with an increase in the supply current the self-inductance is decreasing due to saturation of the iron core, while the mutual inductance is almost constant. The harmonics of the self- and mutual inductances obtained by performing FFT on the measured spatial waveforms of Fig. 5 are listed in Table II. The diagonal and non-diagonal elements in the detailed inductance matrix of the proposed extended *dq* model are calculated from the data of Table II using (38)-(54) as shown in Fig. 6 and Fig. 7, respectively.

According to (74) and (75), harmonics in the *qd0* PM flux linkages and inductances cause ripple in the electromagnetic torque. The prototype FSCW PMSM is designed with the objective of minimum torque ripple; thus, as observed in Fig. 4, Fig. 6 and Fig. 7, the harmonics in the *qd0* PM flux linkages and inductances are relatively small.

B. Prediction of the Average Torque and Torque Ripple

The measured *qd0* parameters for the extended *dq* model are used here to predict the average torque and torque ripple of the prototype machine. The machine is assumed to run at full load under a maximum torque per ampere (MTPA) algorithm. According to (73), only the average values of the *qd0* PM flux linkages and inductances are responsible for

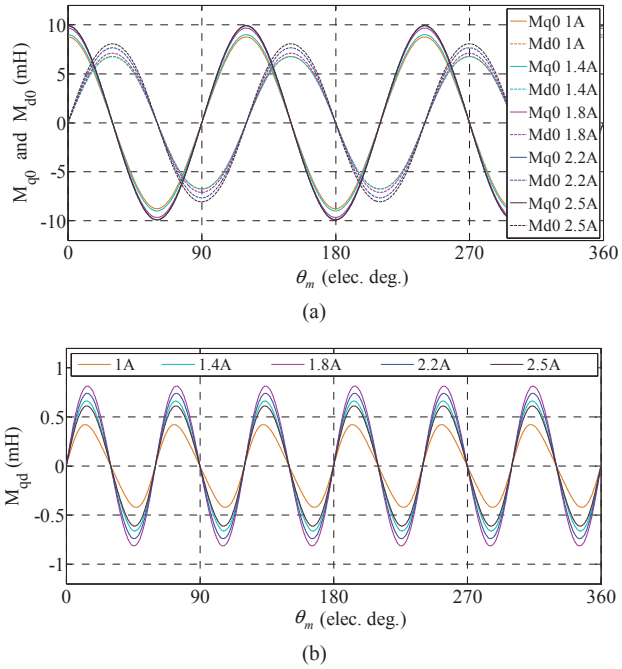

Fig. 7. Non-diagonal elements in the inductance matrix in the proposed extended *dq* model and their variation with current excitation. (a) Mutual inductance between the *d*-axis and 0-axis. (b) Mutual inductance between the *d*-axis and *q*-axis.

generating the average torque. These average values should be used in the MTPA algorithm to obtain i_d and i_q currents, which have the following values at full load: i_q = 3.5A i_d = –0.6A.

In a PMSM the effect of the PM flux linkage harmonics on the torque ripple is dominant and the harmonics in the inductance can be neglected in calculation of the torque ripple [18]. Thus, by assuming negligible inductance harmonics as evident from Fig. 6 and Fig. 7, the developed electromagnetic torque by the prototype machine can be predicted by substituting i_d and i_q in the derived torque

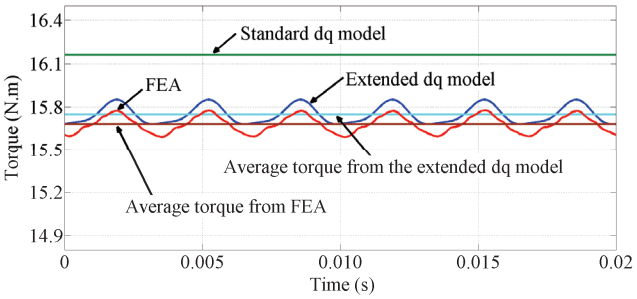

Fig. 8. Predicted electromagnetic torque by the prototype FSCW PMSM vs FEA results

equations, (73)-(75). The results are shown in Fig. 8 for the prototype machine in comparison with the standard *dq* model and the torque obtained from the FEA model of the prototype machine. From Fig. 8 the predicted torque by the proposed model is similar to the torque obtained from the FEA model. The obtained torque ripple by the extended *dq* model is 1.1% of the average torque which complies with the torque predicted by the FEA model. The standard *dq* model is incapable of predicting the torque ripple and returns an average value that is 2.6% higher than the torque predicted by the extended *dq* model.

VI. Conclusion

The detailed model of a non-salient pole FSCW PMSM was derived in the *abc*-system and transferred to the *qd0*-reference frame to form the extended *dq* model. Experimental methods were introduced for measurement of the parameters of the extended *dq* model. The proposed extended *dq* model was further used to formulate the generated torque and torque ripple in the machine. The rigorous mathematical work carried out in this paper showed that the average torque originates only from the fundamental harmonics of the PM flux linkages and self- and mutual inductances. The remaining harmonics of the PM flux linkages and inductances contribute to the torque ripple. Experimental measurements on a prototype FSCW PMSM in the laboratory were performed to obtain the parameters of the proposed extended *dq* model. These parameters were used in the proposed torque model to predict the generated average torque and torque ripple. The obtained results were validated against FEA simulations of the prototype machine.

References

[1] P. C. Krause, O. Wasynczuk, S. D. Sudhoff, and S. Pekarek, *Analysis of electric machinery and drive systems* vol. 75: Wiley, 2013.

[2] T. Sebastian, G. Slemon, and M. Rahman, "Modelling of permanent magnet synchronous motors," *IEEE Trans. Magn.,* vol. 22, pp. 1069-1071, 1986.

[3] H. R. Bolton and R. A. Ashen, "Influence of motor design and feed-current waveform on torque ripple in brushless DC drives," *Proc. Elect. Power Appl.,* vol. 131, pp. 82-90, 1984.

[4] M. Farshadnia, R. Dutta, J. E. Fletcher, K. Ahsanullah, M. F. Rahman, and H. C. Lovatt, "Analysis of MMF and back-EMF waveforms for fractional-slot concentrated-wound permanent magnet machines," in *Proc. ICEM*, 2014, pp. 1976-1982.

[5] L. Alberti, M. Barcaro, and N. Bianchi, "Design of a Low-Torque-Ripple Fractional-Slot Interior Permanent-Magnet Motor," *IEEE Trans. Ind. Appl.,* vol. 50, pp. 1801-1808, 2014.

[6] F. Meier and J. Soulard, "dq theory applied to a permanent magnet synchronous machine with concentrated windings," in *Proc. PEMD*, 2008, pp. 194-198.

[7] A. Chiba, F. Nakamura, T. Fukao, and M. Azizur Rahman, "Inductances of cageless reluctance-synchronous machines having nonsinusoidal space distributions," *IEEE Trans. Ind. Appl.,* vol. 27, pp. 44-51, 1991.

[8] A. Gebregergis, M. H. Chowdhury, M. S. Islam, and T. Sebastian, "Modeling of Permanent-Magnet Synchronous Machine Including Torque Ripple Effects," *IEEE Trans. Ind. Appl.,* vol. 51, pp. 232-239, 2015.

[9] P. Pillay and R. Krishnan, "Modeling, simulation, and analysis of permanent-magnet motor drives. I. The permanent-magnet synchronous motor drive," *IEEE Trans. Ind. Appl.,* vol. 25, pp. 265-273, 1989.

[10] P. Ponomarev, I. Petrov, and J. Pyrhonen, "Influence of Travelling Current Linkage Harmonics on Inductance Variation, Torque Ripple and Sensorless Capability of Tooth-Coil Permanent-Magnet Synchronous Machines," *IEEE Trans. Magn.,* vol. 50, pp. 1-8, 2014.

[11] F. Magnussen and H. Lendenmann, "Parasitic Effects in PM Machines With Concentrated Windings," *IEEE Trans. Ind. Appl.,* vol. 43, pp. 1223-1232, 2007.

[12] R. H. Park, "Two-reaction theory of synchronous machines generalized method of analysis-part I," *AIEEE Trans.,* vol. 48, pp. 716-727, 1929.

[13] G. Dajaku and D. Gerling, "Stator Slotting Effect on the Magnetic Field Distribution of Salient Pole Synchronous Permanent-Magnet Machines," *IEEE Trans. Magn.,* vol. 46, pp. 3676-3683, 2010.

[14] C. Se-Kyo, K. Hyun-Soo, K. Chang-Gyun, and Y. Myung-Joong, "A new instantaneous torque control of PM synchronous motor for high-performance direct-drive applications," *IEEE Trans. Power Electron.,* vol. 13, pp. 388-400, 1998.

[15] L. Yong, Z. Q. Zhu, and D. Howe, "Direct torque control of brushless DC drives with reduced torque ripple," *IEEE Trans. Ind. Appl.,* vol. 41, pp. 599-608, 2005.

[16] I. S. 115A-1987, "IEEE standard procedure for obtaining synchronous machine parameters by standstill frequency response testing," ed, 1987.

[17] L. Chong, R. Dutta, and M. F. Rahman, "Design of a highly efficient 1kW concentric wound IPM machine with a very wide constant power speed range," in *Proc. IPEC*, 2010, pp. 1956-1961.

[18] B. H. Ng, M. F. Rahman, T. S. Low, and K. W. Lim, "An Investigation Into the Effects of Machine Parameters on Torque Pulsations in a Brushless Dc Drive," in *Proc. IECON*, 1988, pp. 749-754.